β-1,3-Glucan polysaccharides as novel one-dimensional hosts for DNA/RNA, conjugated polymers and nanoparticles

Kazuo Sakurai,[a] Kazuya Uezu,[a] Munenori Numata,[b] Teruaki Hasegawa,[b] Chun Li,[b] Kenji Kaneko[c] and Seiji Shinkai*[b]

Received (in Cambridge, UK) 11th May 2005, Accepted 8th July 2005
First published as an Advance Article on the web 3rd August 2005
DOI: 10.1039/b506673p

β-1,3-Glucan polysaccharides have triple-stranded helical structures whose sense and pitch are comparable to those of polynucleotides. We recently revealed that the β-1,3-glucans could interact with certain polynucleotides to form triple-stranded and helical macromolecular complexes consisting of two polysaccharide-strands and one polynucleotide-strand. This unique property of the β-1,3-glucans has made it possible to utilize these polysaccharides as potential carriers for various functional polynucleotides. In paticular, cell-uptake efficiency of the resultant polysaccharide/polynucleotide complexes was remarkably enhanced when functional groups recognized in a biological system were introduced as pendent groups. The β-1,3-glucans can also interact with various one-dimensional architectures, such as single-walled carbon nanotubes, to produce unique nanocomposites, in which the single-walled carbon nanotubes are entrapped within the helical superstructure of β-1,3-glucans. Various conductive polymers and gold nanoparticles are also entrapped within the helical superstructure in a similar manner. In addition, diacetylene monomers entrapped within the helical superstructure can be photo-polymerized to afford the corresponding poly(diacetylene)-nanofibers with a uniform diameter. These findings indicate that the β-1,3-glucans are very attractive and useful materials not only in biotechnology but also in nanotechnology. These unique properties of the β-1,3-glucans undoubtedly originate from their inherent, very strong helix-forming character which has never been observed for other polysaccharides.

[a]*Department of Chemical Processes and Environments, Faculty of Environmental Engineering, The University of Kitakyushu, Hibikino, 1-1 Wakamatsu-ku, Kitakyushu, Fukuoka, 808-0135, Japan*
[b]*Department of Chemistry, Graduate School of Engineering, Kyushu University, Hakozaki, 6-10-1, Fukuoka, 812-8581, Japan*
[c]*The Research Laboratory for High Voltage Electron Microscopy, Kyushu University, Fukuoka, 812-8581, Japan*

1 Introduction

Chinese herbal medicine has a great history extending back to the Late Bronze Age of about 2500 to 3000 years ago. In this long history, some fungi have been recognized as potential medicines to cure gynecological diseases.[1] Modern chemistry has revealed that the active ingredients of these fungi are

Kazuo Sakurai

Kazuo Sakurai was born in 1958 in Gifu, Japan, and after finishing the master's course of Osaka University, he joined Kanebo Ltd in 1984. He spent three years (1990–1993) in the USA working for Prof. MacKnight in the University of Massachusetts, and received a PhD from Osaka University in 1996. He worked for Prof. Shinkai in the JST Project at Kurume from 1999–2001 and he has been a professor of the University of Kitakyushu since 2001.

Kazuya Uezu was born in 1963 in Okinawa, Japan, and received his PhD in 1992 from the University of Tokyo. After Research Associate work at Kyushu University, he became an associate professor at the University of Kitakyushu in 2001. His research interests focus on structural design and elucidation of functional materials for molecular recognition with computational chemistry.

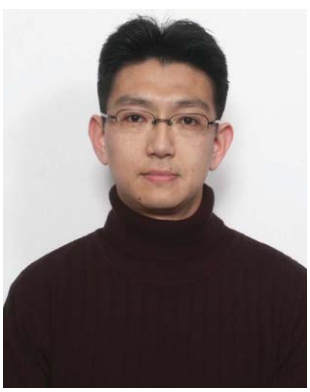

Munenori Numata

Munenori Numata was born in 1970 in Osaka, Japan, and received his PhD in 2000 from Kyushu University under the supervision of Prof. S. Shinkai. After postdoctoral work at the National Institute of Advanced Industrial Science and Technology (AIST), Tsukuba, he joined the JST SORST Project in 2002 as a research fellow. His research interests focus on supramolecular chemistry, bionanomaterials based on DNA and polysaccharides.

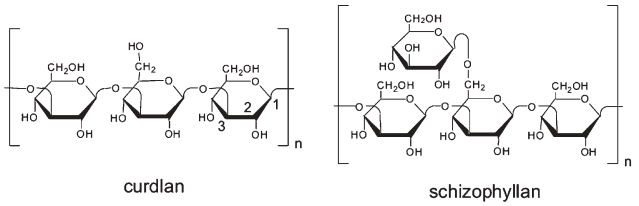

Fig. 1 Chemical structures of curdlan and SPG. The numbers in the figure indicate the atomic numbers of the glycoside unit.

polysaccharides belonging to the β-1,3-glucan family.[2] Among others, schizophyllan (SPG, Fig. 1)[3,4] and lentinan[2] have been commercialized in Japan as medicines for the treatment of uterine cancer. Immunology showed that these β-1,3-glucans can activate natural immunity by promoting secretion of interleukins.[2] Molecular biology of the β-1,3-glucans has just started, being motivated by recent findings that they are recognized by Toll-like receptors which are key regulators of innate immunity responding to invading microorganisms.[5,6]

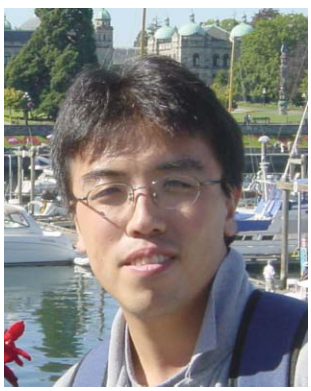

Teruaki Hasegawa

Teruaki Hasegawa was born in 1973 in Mie, Japan, and received his PhD in 2001 from Nagoya University. After postdoctoral work as a JSPS research fellow at the University of Washington with Prof. Tomikazu Sasaki, he joined Kyushu University in 2003 and became a research associate there in 2004. His current research interests focus on carbohydrate and supramolecular chemistry.

Kenji Kaneko

Chun Li received his PhD in 1998 from Nanjing University under the supervision of Professor Yingqiu Liang. He then joined Nanjing University as a Lecturer. From 2001 to 2003 he was a postdoctoral fellow with Professor Toyoko Imae at Nagoya University. In 2003, he moved to Kyushu University as a postdoctoral research associate with Professor Seiji Shinkai. His research interests focus on conjugated polymers and supramolecular chemistry.

Kenji Kaneko was born in 1967 in Gumma, Japan, and received his PhD in 1995 from Bristol University, UK. After returning to Japan, he was employed as a postdoctoral researcher at various institutes, including Tokyo University. After these positions, he joined Kyushu University as an associate professor in 2001. His current research interests focus on characterizing various types of materials by transmission electron microscopy, analytical electron microscopy and three-dimensional electron tomography.

On the other hand, the chemistry of the β-1,3-glucan family has a relatively long history. Atkins[7] and Sarko[8,9] showed that the simplest β-1,3-glucan, or curdlan (Fig. 1), adopts a triple-stranded helical structure in nature. Norisuye *et al.*[10–12] carefully studied the dilute solution properties of SPG and clarified that it dissolves in water as a triple-stranded helical structure (t-SPG) and in dimethylsulfoxide (DMSO) as single-stranded random coils (s-SPG). Furthermore, once water is added to the DMSO solution, t-SPG is regenerated from s-SPG strands (this process is known as a renaturation process) through inter-stranded hydrophobic interactions and hydrogen bonding.[13] Although the resultant renatured product is not exactly the same as the original rod-like molecules, the local structure is expected to restore the triple-stranded helical structure.[13–15]

In 1999, we mixed various biomaterials with s-SPG to examine whether the renaturation process of SPG would be interfered with by the additives. During these experiments, we unintentionally found that s-SPG could form a unique macromolecular complex with poly(C) when poly(C) co-existed during the renaturation process. Later work showed that poly(C) is one of several polynucleotides that are strongly bound to s-SPG and show strong circular dichroic (CD) signals. Fortunately, the poly(C) was left by someone in our refrigerator a few years ago and that was why we used poly(C) in our experiments as a representative of polynucleotides. If we had selected other polynucleotides, such as poly(G), as our initial target, this unique polysaccharide–polynucleotide interaction would not have been discovered (poly(G) is not able to interact with s-SPG, as shown in Table 1). In this sense, this finding is surely an example of scientific serendipity. Since then we have dedicated our research effort to explore this novel polysaccharide/polynucleotide complex and to establish a new method to deliver DNA by using this complex. The present review summarizes our tidemark in recent work.

Seiji Shinkai

Seiji Shinkai was born in 1944 in Fukuoka, Japan, and received his PhD in 1972 from Kyushu University, where he became a lecturer soon afterwards. After postdoctoral work at the University of California, Santa Barbara with Thomas C. Bruice, he joined Kyushu University in 1975 and became a full professor there in 1988. His research interests focus on host–guest chemistry, molecular recognition, sugar sensing, allosteric functions, organogels, sol-gel transcription, polysaccharide–polynucleotide interactions, etc.

Table 1 Nucleotide specificity in complex formation in natural and non-salt aqueous solution

		Complex formation	T_m/°C	Conformation
RNA	Poly(C)	Yes	54	Single chain
	Poly(A)	Yes	32	Single chain
	Poly(U)	No		Intramolecular H-bond (hairpin like)
	Poly(G)	No		4G wire (intramolecular H-bond)
	Poly(I)	No		Intramolecular H-bond
DNA	Poly(dC)	No		Intramolecular H-bond
	Poly(dA)	Yes	(40)[a] 80	Single chain
	Poly(dT)	Yes	10	Single chain
	Poly(dG)	No		4G wire (intramolecular H-bond)

[a] Conformational transition temperature, see the text for detail.

2 Structural aspects of the triple-stranded helical structure of β-1,3-glucans[16]

One of the most characteristic features of the structure of β-1,3-glucans is that they adopt a right handed 6_1 triple-stranded helical structure in nature. X-ray crystallography has already been extensively carried out to find that curdlan also adopts a 6-fold, parallel, triple-stranded helical structure.[9,17] The X-ray diffraction pattern, however, provides the atomic coordinates for carbon and oxygen but not for hydrogen and therefore, the hydrogen bonding to maintain the triple-stranded helical structure has not been clarified. One possible and widely believed model is the helical structure stabilized through inter-stranded hydrogen bonding among the three O2 atoms, as shown in Fig. 2a.[7,9] Here, the upper model shows a side view of the helical structure and the lower schematic illustration presents a cross section by projecting all atoms to the *x*–*y* plane (perpendicular to the *c*-axis). Three 2nd hydroxyl groups protrude toward the centre of the helical structure and form a closed triangle hydrogen-bonding network. Since each triangle hydrogen-bonding network employs three hydroxyl groups that are located in the same *x*–*y* plane along the helical structure, it is arranged perpendicular to the helix axis, as presented in the upper panel.

Recently, we re-examined the hydrogen-bonding stabilizing the triple-stranded helical structure of curdlan by using semi-empirical quantum-mechanics (MOPAC). The result of our calculation showed a possibility that the triple-stranded helical structure could be stabilized through unique "continuous" hydrogen-bonding networks (Fig. 2b) along the helical structure.[16] In the newly proposed model, three single-strands of curdlan are connected by inter-stranded hydrogen-bonding networks among oxygen atoms (O2 and O2′) on different *x*–*y* planes.

In the case of the triangle hydrogen-bonding networks, our semi-empirical calculation revealed that the triple-stranded helical structure of curdlan is stabilized by the hydrogen bonding in an almost independent manner from the unit number (or molecular size of curdlan), due to discontinuity in the triangle hydrogen-bonding networks. On the other hand, the stability is increased with increasing unit number for the newly proposed continuous hydrogen-bonding networks. This feature can be explained by a combination of electron-induced effect and charge-transfer effect along the continuous hydrogen-bonding networks, which can be called cooperative phenomena characteristic of polymer systems. It should be emphasized that the continuous network model becomes more stable than the original triangle one when the unit number exceeds 10.

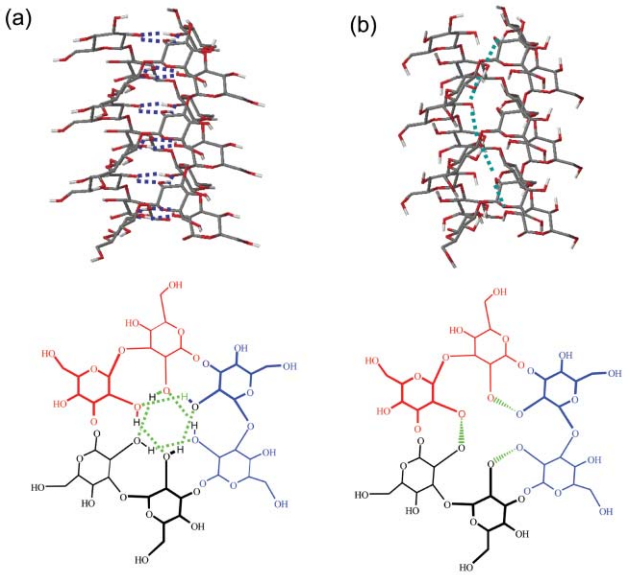

Fig. 2 Proposed two types of hydrogen bonds in curdlan triple helix. (a) The hexagonal intermolecular hydrogen bonds. The upper model is a side view of the full turn triple helix, here the dotted lines indicate the hydrogen bonds, and the lower one is a cross-sectional view of the helix (perpendicular to the helix). (b) The left-handed helical hydrogen bonds. The side view and cross-sectional view are presented in the same manner as in panel (a). The hydrogen bonds are connected along the helix, traversing three curdlan chains to make a left-handed helix. Therefore, the hydrogen bond array makes a reverse helix of the main chain.

3 Complexation between the β-1,3-glucans and polynucleotides

3.1 Spectroscopic changes upon complexation[18,19]

Fig. 3 compares the ultraviolet absorbance (UV) and CD spectra of poly(C)† itself and that complexed with s-SPG (the macromolecular complex is denoted as poly(C)/s-SPG). Here the M_w of s-SPG is 150 K and the base number of poly(C) is about 250. The complexation induced several changes in the UV and CD spectra of poly(C), that is, 1) a decreased UV absorbance (270 nm) by 12% (hypochromism), 2) an increased CD (275 nm) signal and 3) a newly-appeared CD band (245 nm). Since SPG does not have any functional group to absorb light in this wavelength range, the hypochromism of UV should arise from intensified base-stackings through the

† Hereinafter, poly(X) denotes a homo-polynucleotide and X is the base symbol such as A (adenosine monophosphate), C (cytidine monophosphate), G (guanosine monophosphate), U (uridine monophosphate), I (inosine monophosphate), dA (deoxyadenosine monophosphate), *etc*.

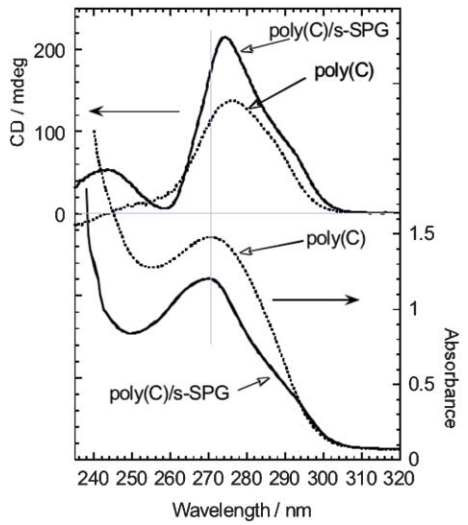

Fig. 3 Comparison of the UV and CD spectra between poly(C) and poly(C) + s-SPG measured at 10 °C for a concentration of poly(C) of 7.16×10^{-3} g dL^{-1} (2.22×10^{-4} M) with a 1 cm cell. (Adapted from ref. 19 by permission of The American Chemical Society).

complexation. Furthermore, the increment of CD after the complexation implies that poly(C) takes a highly ordered helical structure after the complexation, and the content of the helical structure (or an ordering of it) is increased. Along with these spectral data, we assumed that the complexation induced a new ordered helical structure of poly(C). This SPG-induced ordered structure is clearly different from random aggregations induced by polycation–polynucleotide interactions, through which the CD spectra are usually depressed.

Table 1 summarizes the macromolecular complex formation between s-SPG and homo-polynucleotides in natural and non-salt aqueous solution. Poly(C), poly(A), poly(dA) and poly(dT) can form a macromolecular complex with s-SPG, although poly(G), poly(U), poly(I), poly(dG) and poly(dC) show no affinity toward s-SPG. According to the previous work,[22] poly(G) and poly(dG) form tetramers, poly(U) and poly(dC) form dimers and poly(I) forms a tetramer or trimer. In these cases, the hydrogen-bonding sites in the bases are occupied by intra- or inter-molecular interactions. On the other hand, poly(C), poly(A), poly(dA) and poly(dT) do not form such superstructures, and therefore their hydrogen-bonding sites are unoccupied. There is a clear correlation between the complexation ability and the presence of free hydrogen-bonding sites, *i.e.*, the polynucleotides having free hydrogen-bonding sites can form macromolecular complexes with s-SPG. This correlation also clearly indicates that the hydrogen bonding between s-SPG and polynucleotides is essential to induce the macromolecular complex formation.

We examined whether the other glucans would show similar UV- and CD-spectral changes when they were treated with poly(C) in the same manner as SPG (*i.e.*, dissolved or dispersed in DMSO and the solvent exchanged for water in the presence of poly(C)). The results summarized in Table 2 indicate that the complexation is only observed for the β-1,3-glucans. It should be emphasized that the natural triple-stranded helical structure of SPG (t-SPG) cannot induce any CD and UV

Table 2 Relationship between the capability to form the complex and the glucose linkage of natural glucans

Name	Units	Linkage	Side chain	
Amylose	α-D-Glucose	1,4	none	No
Carrageenan	β-D-Galactose	Alternating 1,4 and 1,3	Sulfonic groups	No
Cellulose	β-D-Glucose	1,4	none	No
Dextran	α-D-Glucose	1,6	α-1,3- or α-1,4-	No
Pullulan	α-D-Glucose	1,6	none	No
Lentinan	β-D-Glucose	1,3	-G(-G)-G-G(-G)-	Yes
Curdlan	β-D-Glucose	1,3	-G-G-G-G-G-	Yes
Schizophyllan	β-D-Glucose	1,3	-G-G(-G)-G-	Yes

spectral change of poly(C), suggesting it has no affinity for poly(C). This fact clearly shows that the renaturation process is indispensable for the complexation.

Fig. 4 presents the temperature dependence of $[\theta]_{max}$ for free homo-polynucleotides and their macromolecular complexes with s-SPG, where $[\theta]_{max}$ is a maximum CD-intensity at the top of their positive bands. As seen in Fig. 4, there is an abrupt decrease in $[\theta]_{max}$ around 32 and 54 °C for s-SPG/poly(A) complex and s-SPG/poly(C) complex, respectively. Furthermore, above each critical temperature, the $[\theta]_{max}$ of these complexes merges into those of the corresponding free polynucleotides themselves. These features show that s-SPG/polynucleotide complexes can be formed only under a low temperature range and they are dissociated (or melt) upon heating. It is of interest that the abrupt decrease resembles a well-known melting behavior of polynucleotide-based double-stranded helices.

As summarized in Table 1, melting temperatures (T_m) evaluated from the plots show a clear difference between those for s-SPG/poly(C) complex and s-SPG/poly(A) complex. This difference is also of great interest since a similar tendency in T_m can be observed for the corresponding polynucleotide-based double-stranded helices, that is, poly(C)/poly(G) complex "melts" at a higher temperature (*ca.* 110 °C) in comparison to poly(A)/poly(U) complex (*ca.* 65 °C). The

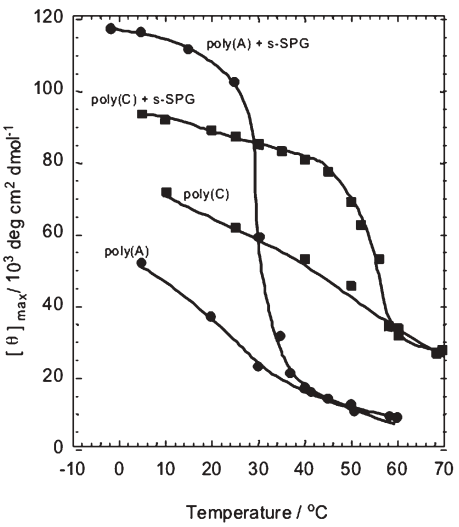

Fig. 4 Temperature dependence of $[\theta]_{max}$ for poly(A) and poly(C), and their mixtures with s-SPG.

different T_m values observed for the DNA helices can be ascribed to the difference in the number of the hydrogen bonds (cytosine has 3 hydrogen-bonding sites whereas adenosine has 2 sites). The same debate can also be applied to the difference in T_m values between s-SPG/poly(A) complex and s-SPG/poly(C) complex, supporting our assumption that the hydrogen bonding is essential for the macromolecular complex formation.

Fig. 5 plots relative CD-intensities against V_w for both poly(A) and poly(C) systems. Here, V_w is a volume fraction of water in the water/DMSO mixed solution and the relative CD-intensity is defined as normalized $[\theta]_{max}$ based on that of poly(A) or poly(C) at $V_w = 1$. In the low V_w region, the individual polynucleotide exhibits the same values as the corresponding mononucleotide, indicating no or negligibly weak base-stacking along the polynucleotide-strands. The relative CD-intensities commence to increase at $V_w = 0.5$ for poly(A) and at $V_w = 0.6$ for poly(C). These increments indicate that the polarity of the solvent becomes significant enough to induce the hydrophobic interaction and the resultant base-stacking. The relative CD-intensities are then increased essentially linearly with increasing V_w for both polynucleotides. On the other hand, when s-SPG coexists, polynucleotides show completely different behaviour from that of the corresponding free polynucleotides. In the lower V_w region (*ca.* 0.00–0.45), the relative intensities stay at the same values as those of the corresponding mononucleotides. The intensities increase dramatically at $V_w = 0.58$ for poly(A) + s-SPG and at $V_w = 0.60$ for poly(C) + s-SPG, and are then saturated at $V_w > 0.70$. The onset V_w values for the macromolecular complex formation are close to the V_w values at which the base-stacking of poly(A) and poly(C) begins. This coincidence indicates that the hydrophobic interaction between the bases is a key feature to induce the macromolecular complexation. Furthermore, the saturation of relative CD-intensities indicates that most of the bases are stacked under high V_w conditions ($V_w > 0.7$) and that the macromolecular complex formation is completed under these conditions.

We prepared three s-SPG samples with M_w = 2100, 3800 and 7200 through acid hydrolysis of native SPG (M_w = 15000) to investigate its suitable molecular weight to form the macromolecular complex with poly(C) (the base number of poly(C) was fixed at 250). We also examined how many bases in the polynucleotides are required for the macromolecular complexation by using various poly(dA) samples having different base numbers and s-SPG having a fixed molecular weight (15000). It is found that the critical M_w of s-SPG for the macromolecular complexation is 3000–5000, indicating that *ca.* 16–30 glucose units are required for the complexation. On the other hand, 25–30 deoxyadenosine units are required to combine with the s-SPG.

3.2 Stoichiometry and molecular modeling[18–20]

We measured the CD spectra of poly(C) by changing the molar ratio between polynucleotides and s-SPG to determine the stoichiometry in the macromolecular complex. As shown in Fig. 6, the $[\theta]_{max}$ value increases linearly with increasing molar ratio (defined in the legend of Fig. 6), following an upward convex, and finally stabilizes at about 0.4. From the cross section of the plateau and increment regions, the stoichiometric ratio (N) is evaluated to be 0.38–0.42.[19] This result indicates that two SPG repeating units are combined with three base units, namely, 8 glucoses *vs.* 3 bases. When we examined the stoichiometry for the curdlan/poly(C) system, the results showed 6 glucoses *vs.* 3 bases.[21] Together with the fact that curdlan has no side chain and SPG has one glucoside side chain, this discrepancy in the stoichiometric ratios can be rationalized by assuming that the main chain of the β-1,3-glucans participates in the complexation whilst the side chain of SPG is not involved in the complexation.

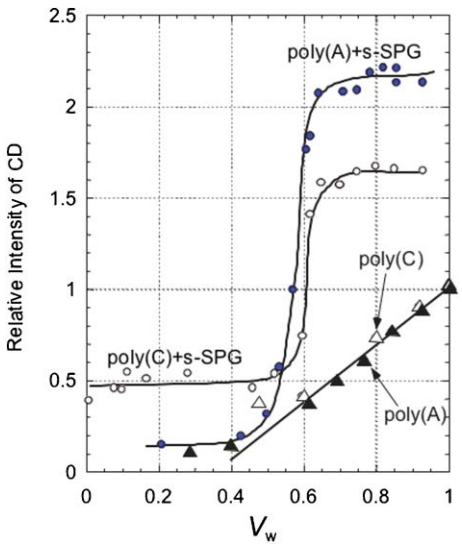

Fig. 5 Composition dependence of the relative intensity of CD for poly(C), poly(C) + s-SPG, poly(A) and poly(A) + s-SPG. (Adapted from ref. 19 by permission of The American Chemical Society).

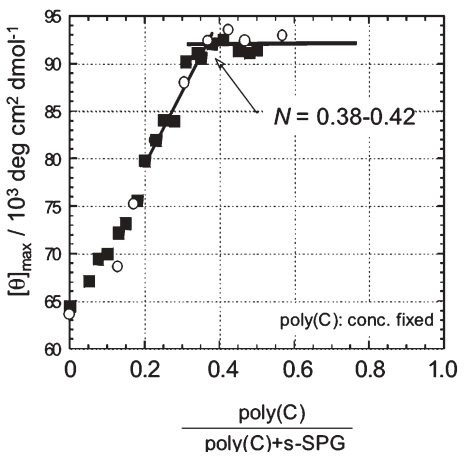

Fig. 6 The Job plot for the poly(C) + s-SPG system. The molar ratio is defined by $M_{s\text{-}SPG}/(M_{s\text{-}SPG} + M_{poly(C)})$, where $M_{s\text{-}SPG}$ and $M_{poly(C)}$ are the molar concentrations of s-SPG and poly(C), respectively. The cross section of the plateau and increment regions shows that the stoichiometric ratio = 0.38–0.42. (Adapted from ref. 19 by permission of The American Chemical Society).

We can speculate on a few possible structures based on the facts that: 1) the second hydroxyl groups should be involved in the macromolecular complex formation because they participate in the hydrogen bonding to stabilize the original triple-stranded helical structure of β-1,3-glucans, 2) the glucoside side chain is not involved in the macromolecular complex formation and 3) the resultant macromolecular complexes have highly regular helical structures as supported by the CD and UV spectral data.

Fig. 7 illustrates the three possible structures for the curdlan/poly(C) complex. In Model D1, every glucose residue in the main chain interacts with the cytosine residue to form a DNA-like double helix. Since the distance between the neighbouring C-2 carbons is about 4 Å and the stacking distance between cytosine moieties is 3.0–3.6 Å, this model is reasonable from the viewpoint of the stereochemistry. The stoichiometric number ($N = 0.20$) of Model D1, however, does not agree with the experimental results in Fig. 6. We therefore constructed another double-stranded model (D2 in Fig. 7) to satisfy $N = 0.40$, however, the ribose or phosphate moieties are unfavourably stretched and thus this model is also not acceptable. In Model T1, we suppose that the macromolecular complex adopts a triple-stranded helical structure similar to the original triple-stranded helical structure of curdlan. When we construct the helical structure from two s-SPG chains and one poly(C) chain, this model can satisfy both the stereochemistry and the stoichiometry ($N = 0.40$). Model T1 is, therefore, the most suitable one to reasonably explain all the experimental results.

Based on the above stoichiometric discussion, we constructed a three-dimensional (3D) model of the macromolecular complex. We first constructed the triple-stranded helical structure of curdlan and removed one strand from this helical structure. Secondly, we created a single-stranded helical structure of poly(C) based on its crystal structure[22] and merged it with the double-stranded helical structure of curdlan. In fact, the resultant "hybrid-type" helix composed of the two curdlan strands and one poly(C) strand could be easily constructed due to their similar right-handed 6_1 helical structure. In the third step, we calculated the most stable conformation of poly(C) confined in the groove using a MOPAC MM3 in CAChe, version 5 (Fujitsu, Ltd, Japan). The calculation was converged to indicate that the poly(C) strand can adopt a conformation that is very close to the original one without creating any steric hindrance.[20] The obtained model is shown in Fig. 8(a). Interestingly, the cytosine units are located close to the 2nd hydroxyl groups to form hydrogen bonding as presented in panel (b). The 3rd and 4th nitrogen atoms in the cytosine units participate in intermolecular hydrogen bonding and the resultant "hybrid-type" cytosine–glucose hydrogen bonding replaces the original hydrogen bonding in the triple-stranded helical structure of curdlan.

An enthalpy change (ΔH) through the macromolecular complexation can be defined by

$$\Delta H = 3H_{complex} - (3H_{poly(C)} + 2H_{curdlan3}) \quad (1)$$

where $H_{complex}$, $H_{poly(C)}$ and $H_{curdlan}$ are the calculated heat of formation (HOF) for the curdlan/poly(C) complex, the poly(C) single strand and the curdlan triple-stranded helix, respectively. In the calculation, we considered a set of two glucose and one cytosine residues as an elemental unit and divided the ΔH by the unit-number (ΔH/unit). With this normalization, we can easily compare the ΔH between the different chain lengths. Fig. 8(c) shows the relationship between the chain length and the ΔH/unit. When the ΔH/unit is positive, the macromolecular complex formation is a thermodynamically less favourable process than the formation of the curdlan triple-stranded helical structure. It should be noted that the ΔH/unit decreases with increasing chain length, and turns negative at around 24 units. This result is consistent with our experimental results showing that polynucleotide having more than 30 nucleobase-units can form stable macromolecular complexes with s-SPG.[19]

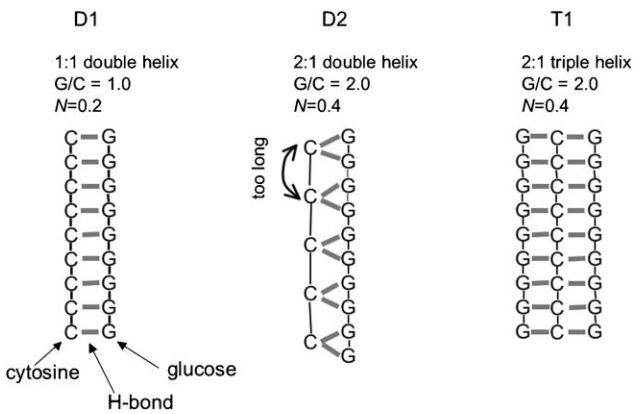

Fig. 7 Three possible structures for the s-SPG/poly(C) complex. G and C denote the glucose and cytosine in the chains, respectively. In Model D1, every glucose residue in the main chain interacts with the cytosine. Model T supposes that the complex adopts a triple helix similar to that existing in the β-1,3-glucans.

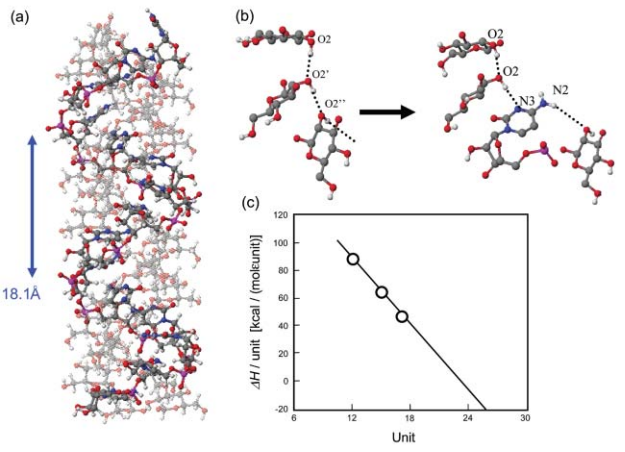

Fig. 8 The curdlan/poly(C) complex calculated by MOPAC. (a) A full turn model of the side view, the curdlan double helix is translucent and the pitch of poly(C) is 18.1 Å. (b) Hydrogen bonds between the curdlan and the poly(C) in the complex. (c) The ΔH per unit of complex is plotted against the unit number.

4 Application to biotechnology

4.1 Specific binding to natural mRNAs[23]

We have found that s-SPG is capable of specifically interacting with various mRNAs by the following experiments. We first synthesized SPG having appended fluorophores through treating native SPG with fluorescein 4-isothiocyanate and then, the degree of fluorescence polarization (*P*) was measured after mixing with mRNA from *Saccharomyces cerevisiae* (Fig. 9). An addition of mRNA strongly increases the *P* value, while the other RNAs (rRNA and tRNA) do not induce any change in the *P* value. Generally, it is widely recognized that the *P* value increases with increasing molecular weight, owing to a suppressed rotational diffusion coefficient. The present results, therefore, clearly indicate that s-SPG can selectively interact with mRNA to form a macromolecular complex having an increased total molecular weight. This selectivity toward mRNA can be rationalized by the fact that mRNA has a poly(A)-tail which forms the stable macromolecular complex with s-SPG. On the other hand, the other RNAs have no poly(A)-tail and therefore, no s-SPG affinity can be expected. It should be emphasized that, although there are some proteins which can bind to mRNA, most proteins utilize electrostatic interactions to recognize polynucleotides and therefore no mRNA-selectivity can be expected for these proteins. On the contrary, s-SPG does not utilize the non-specific electrostatic interaction but the specific macromolecular complex formation to interact with mRNA. Taking this advantage of s-SPG, we recently prepared an SPG-appended gel column and demonstrated that this column can separate mRNA from crude mixtures extracted from cells.[24]

4.2 Delivery of functional oligonucleotides

4.2.1 Bio-functional oligodeoxynucleotides and their potential carriers. Oligodeoxynucleotides (ODNs) containing an unmethylated CpG sequence (CpG motif) have been shown to stimulate an immune response.[25] Considerable attention is currently devoted to this response because the CpG motif can be an extraordinarily effective adjuvant for many vaccines against infectious agents, cancer antigens and allergens. Henmi *et al.*[26] demonstrated that CpG motifs are recognized by a pattern-recognition receptor, called Toll-like receptor 9 (TLR-9). Recently, TLR-9 was found to be localized in endosome and lysosome compartments.[27] These findings suggest that, if the CpG motifs can be delivered to these organelles with appropriate carriers, the immune response can be artificially and more accurately controlled in comparison to its naked administration. Such carriers should be capable of 1) protecting the complexed CpG motifs from enzymatic degradation and 2) releasing the complexed CpG DNA at the target organelles.

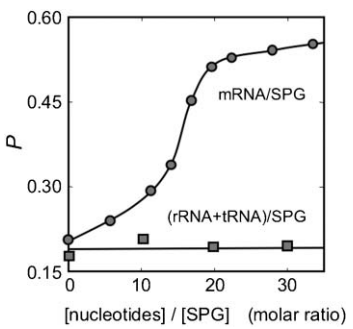

Fig. 9 Comparison of the fluorescence depolarization between mRNA + s-SPG and tRNA/rRNA + s-SPG.

In addition to the CpG motifs, antisense oligonucleotides (AS ODNs) are also functional ODNs of great interest and designed to suppress expressions of particular genes. In spite of their great therapeutic potential, enzymatic degradation by human nucleases strongly hinders their therapeutic applications. Effective methodologies to protect AS ODNs from enzymatic degradation should be, therefore, developed to establish practical antisense therapy. The degradation can be overcome by using ODN analogues, such as phosphorothioates, phosphoramidates and peptide nucleic acids. The phosphorothioate-type ODNs are the leading candidates among the first-generation antisense compounds, however, those analogues are easily absorbed by serum proteins, causing an unfavourable lowering of the antisense efficiency.[28] Although various synthetic polycations including poly-(L-lysine) and polyethyleneimine have been developed as artificial carriers to protect the complexed AS ODNs from the unfavourable binding to the serum proteins, the toxicity of these polycation-based carriers as well as the poor solubility of the resultant carrier/AS ODNs complexes still strongly hinders their wide application for practical antisense therapy.[29]

4.2.2 Strategy and chemistry. Fig. 10 schematically presents the target organelles for the functional oligonucleotides. Native SPG having no cell binding site is unable to bind to the plasma membrane and to induce the following endocytosis. It is, therefore, an important requirement to develop SPG

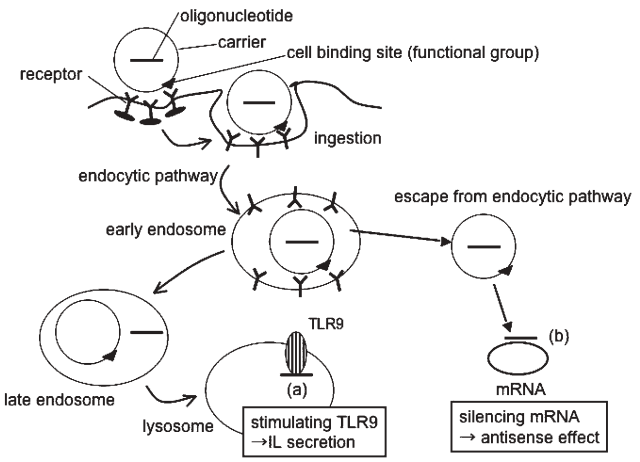

Fig. 10 Our strategy to deliver oligonucleotides to cells. A functional group that can induce the cellular uptake of the complex is attached to the s-SPG side chain. When the modified s-SPG and oligonucleotide are mixed, they form a complex consisting of two modified s-SPG chains and one nucleotide chain. Once the functional group binds to the plasma membrane, cellular uptake can be induced to ingest the complex. Final target organs for antisense DNA and CpG motif. The target of antisense is mRNA, located in the cytosol, and that of the CpG motif is TLR-9, located in the lysosome.

derivatives having cell binding sites to induce effective cellular uptake. To develop such SPG-based carriers, only the side chain of SPG is required to be modified, because structural modifications and the resultant conformational disorders of the β-1,3-glucan main chain should result in a destabilization of the resultant macromolecular complexes.

Fig. 11 presents our synthetic strategy, through which the site-specific modification can be achieved. Native SPG was first oxidized with $NaIO_4$ to yield SPG carrying formyl-appendages. Since the $NaIO_4$-oxidation is specific for 1,2-diols, the SPG main chain having no 1,2-diol remains unmodified through this reaction. The subsequent reductive amination afforded SPG having various functional groups on the side chains.[30,31] We synthesized various SPG-derivatives through this synthetic scheme as listed in Table 3. In addition to the inherent advantages of SPG to protect the complexed ODNs from the nuclease-mediated hydrolysis and from the unfavourable binding to the serum proteins,[32,33] cell affinity

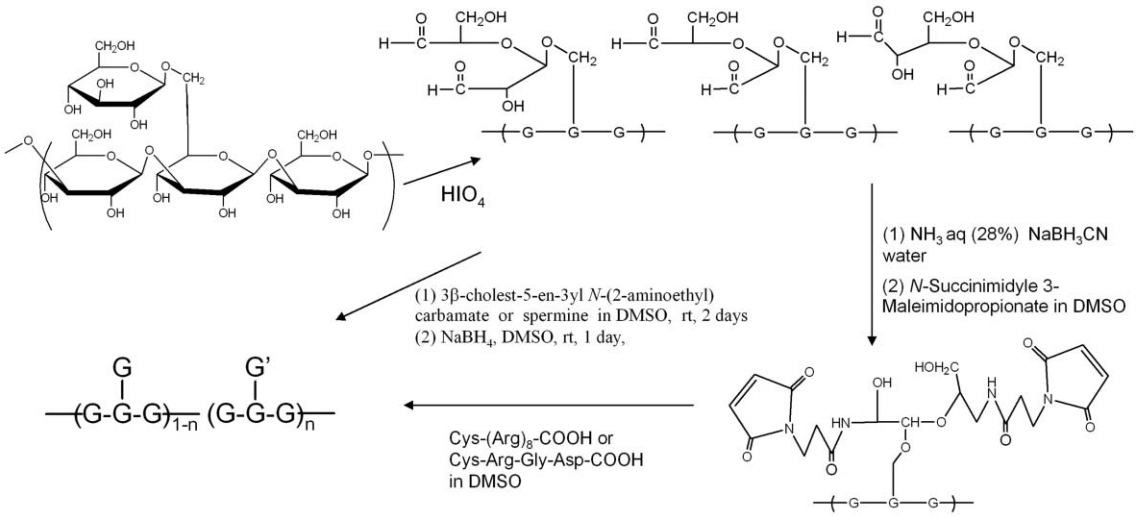

Fig. 11 Schematic presentation to introduce various functional groups to the side chain of SPG.

Table 3 Sample codes and the introduced chemical groups

Sample code	R	Modification level[a]	N/P ratio[b]
SP-SPG	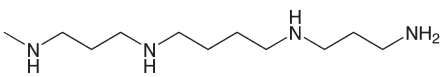	4.6 ± 0.3 mol %	0.27
Chol-SPG	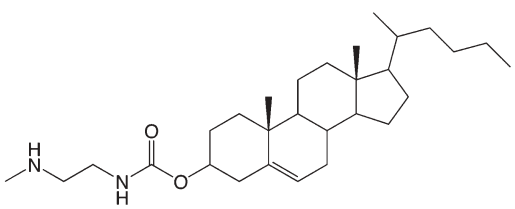	6.9 ± 1.0 mol %	0.21
R8-SPG	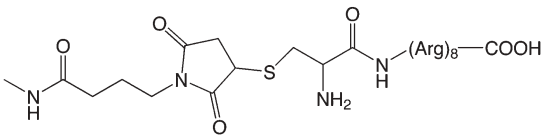	0.5 ± 0.1 mol %	~0
RGD-SPG	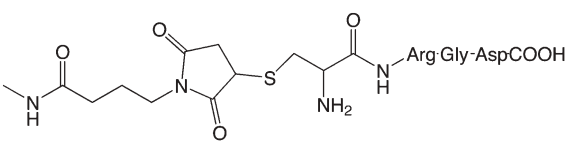	1.3 ± 0.3 mol %	~0

[a] Determined by N elemental analysis. [b] Cation (N)/anion (P) ratio. (Adapted from ref. 34 by permission of The American Chemical Society)

arising from the appended cell binding sites increases the total antisense efficiency of the resultant complexes.

After ingestion by cells, the functional ODNs (AS ODNs and CpG DNA) should be delivered to the specific sites where their targets exist. For example, the AS ODNs should be released from the endocytic pathway to bind the target mRNA, which is present in the cytosol. This event should preferably happen before the AS ODNs start to suffer from enzymatic degradation in the lysosomes. On the other hand, CpG motifs have to be released from the carrier either in the lysosome or late endosome, because the receptor for CpG motifs is located in these organelles.

4.2.3 Delivery of CpG motifs[34]. Fig. 12 shows the comparison of cytokine secretion between the naked dose of CpG DNA and the carrier-mediated ones. When the complex consisting of native SPG and CpG DNA (s-SPG/CpG DNA) was added, secretion was increased by about 20–40% in comparison to that of the naked dose. This increment can be ascribed to the SPG-mediated protection effect of the complexed CpG DNA from the nuclease-mediated hydrolysis. The CpG DNA complexed with the chemically-modified SPG-derivatives increases the secretion dramatically, *i.e.*, five- to ten-fold compared with that of the naked dose. Among these SPG-derivatives, R8-SPG had the highest performance as the carrier, followed by RGD-SPG and then Chol-SPG. The difference in the performance between RGD-SPG and Chol-SPG was prominent for IL-6 but relatively small for IL-12 and TNF-α.

The cellular ingestion mechanisms depend on the chemical structure of the carriers. The cellular membrane is negatively charged, so that cations such as monomeric spermine can bind to the surface *via* coulombic forces and are then ingested by pinocytosis. While this mechanism should be the case for free SP-SPG, ingestion *via* an electrostatic interaction does not occur for the SP-SPG/CpG DNA complex because it has total negative charge (see Table 1). This cancellation of inherent positive charge on macromolecular complexation should be the reason why SP-SPG is not effective as the carrier.

On the other hand, monomeric RGD or monomeric cholesterol is thought to be ingested *via* ligand–receptor interactions. This receptor-mediated ingestion should be also the case for the CpG DNA complexed with RGD-SPG or Chol-SPG and therefore, should be a critical step for their relatively high secretion inductions. After this receptor-mediated ingestion, the RGD-SPG/CpG DNA complex and Chol-SPG/CpG DNA complex would be transported into the endosome and finally into the lysosome, in which the compartment pH is maintained at about 5 and digestive enzymes are highly activated. The complexes should release the CpG DNA owing to the low pH and the resultant naked CpG DNA is easily hydrolyzed into the fragments that are finally recognized by TLR-9 on the vesicle membrane.

It should be noted that the complexes based on the SPG-derivatives having arginine-rich peptides, such as R8-SPG, should be ingested through a different pathway from that based on RGD-SPG and Chol-SPG. Although there is still controversy and some discussion on the uptake mechanism for monomeric R8, some data suggest that R8 is ingested by the cell through a pathway independent from lysosomes and endosomes. If this non-lysosomal pathway was the sole one for the R8-SPG complex, the resultant cytokine secretion would be less than that obtained for the other complexes. The R8-SPG complex, however, induced the highest level of secretion—almost ten times higher than that obtained with naked CpG DNA. To the best of our knowledge, this enhancement is the strongest one achieved through artificial carriers so far reported. The precise mechanism for the ingestion of R8-SPG/CpG DNA complex and the resultant effective cytokine secretion remains to be clarified.

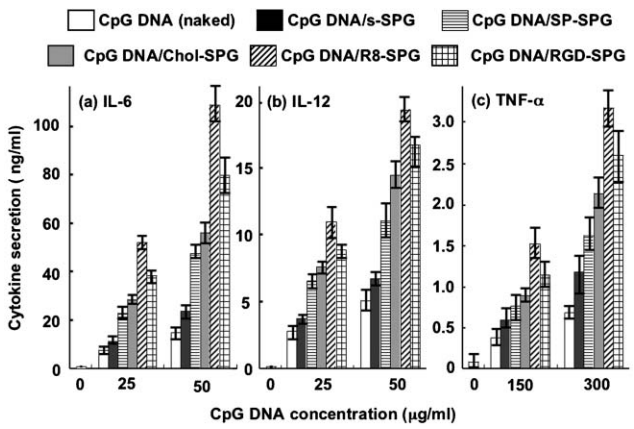

Fig. 12 Effect of chemical modification of s-SPG on CpG-motif-mediated cytokine secretion. The murine macrophage-like cell J774.A1 (1×10^6 cells/ml, 100 μl/well) was stimulated with IL-6 and IL-12 at 25 and 50 μg/ml, and with TNF-μ at 150 and 300 μg/ml. (Adapted from ref. 34 by permission of The American Chemical Society).

4.2.4 Delivery of antisense DNA[30,32,33,35,36]. The same chemical modifications as described in the section 4.2.3 were used to design a carrier for AS ODNs. Several SPG/AS ODNs complexes were prepared and then used for an antisense assay, in which phosphorothioate AS ODN was administered to melanoma A375 or leukemia HL-60 cell lines. The R8-SPG or RGD-SPG could mediate the strongest antisense effect (Fig. 13), most likely due to the enhancement of endocytosis by the functional peptide-appendages. It should be emphasized that the tendency observed in the antisense assay is clearly consistent with that observed in the aforementioned CpG assays. These results clearly support the view that the SPG derivatives having cell binding appendages are potential ODNs-carriers not only protecting the therapeutic ODNs from nonselective protein adsorption and enzymatic degradation but also enhancing the cell-uptake efficiency.

5 Application as unique one-dimensional hosts

It is already known that the 2nd hydroxy groups and the surrounding structure along the β-1,3-glucan main-chain form a more hydrophobic site in comparison to that of primary hydroxy groups or β-1,6-glucoside-appendages.[16] This hydrophobic site, therefore, forms a hydrophobic cavity within the helical superstructure of SPG when s-SPG retrieves its original

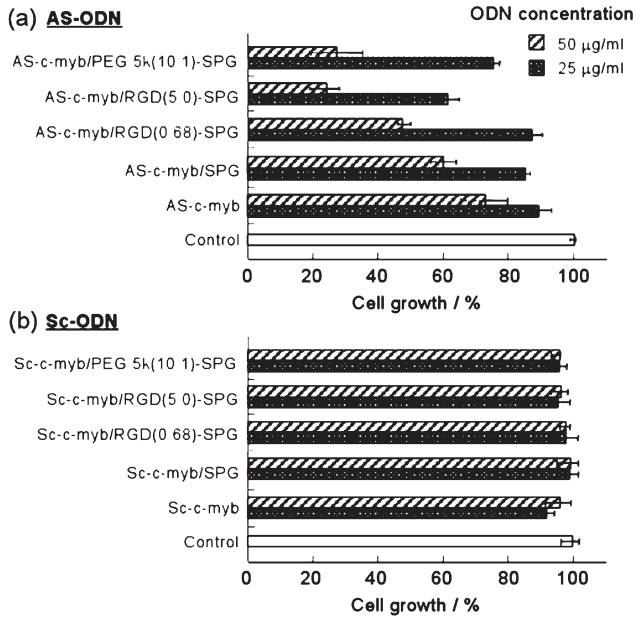

Fig. 13 Comparison of cell growth when A375 cells were exposed to AS-c-myb and the complexes with s-SPG or PEG 5K(10.1)-SPG, RGD(5.0)-SPG and RGD(0.68)-SPG. (a) AS-c-myb assays, (b) Sc-c-myb assays.

triple-stranded helical structure in aqueous media. This unique amphiphilic core-shell structure resembles that of cyclodextrins and therefore, SPG can be considered as a cylindrical, or one-dimensional (1D) analogue of cyclodextrins which are well-established hosts and mainly bind small spherical compounds.[37] This idea encouraged us to pursue the possibility that SPG could act as a novel 1D host, in which various guests are accommodated to provide the corresponding linear assemblies. In the course of our research, we have found several successful examples of SPG-based 1D hosts accommodating various guest molecules including not only polymeric guests but also small compounds as well as nanoparticles to produce unique fibrous assemblies of these entities.

5.1 Inclusion of SWNTs[38]

Since the discovery of single-walled carbon nanotubes (SWNTs),[39] they have been expected to be a new potential framework for advanced materials.[40,41] However, their strong cohesive nature and poor solubility have long been troublesome for researchers, because these properties are seriously obstructive in the search to obtain reproducible data. One potential solution to overcome these problems is to solubilize SWNTs through composite formation with various water-soluble polymers. So far, several research groups have demonstrated that certain natural polymers have a potential ability to interact with SWNTs, making it possible to prepare their water-soluble composites.[42] Among them, natural polysaccharides including amylose reported by Stoddart's and Kim's groups[43] are of great interest because: 1) they have almost no light absorption in the UV-VIS wavelength region so that the dispersed composites are very suitable for photochemical experiments, 2) the sugar-coated surface of the resultant composite should be bio-compatible and therefore, they would be applicable for various medicinal purposes and 3) if the sugar group is recognized by carbohydrate-binding proteins (lectins), one can construct novel SWNTs-based supramolecular network structures.[44]

As described in the previous sections, the major driving forces for the re-construction of t-SPG from s-SPG are considered to be the hydrophobic interaction in addition to the hydrogen bonding.[45] It thus occurred to us that SWNTs might be entrapped, owing to the hydrophobic interaction, in the inside hollow of the SPG helical structure. As expected, we have found that s-SPG and s-curdlan are capable of wrapping not only SWNTs cut to 1–2 μm length (c-SWNTs) but also as-grown SWNTs (ag-SWNTs: in some cases, one piece of ag-SWNT) and the "periodical" stripes arising from the twining SPG strands are clearly observable by AFM and TEM, reflecting the strong helix-forming nature of the β-1,3-glucan main chain.

We first studied this system using c-SWNTs because its handling is easier than that of ag-SWNTs. SWNTs were cut to the appropriate length as described previously.[46] Fig. 14 shows a VIS-NIR spectrum of the s-SPG/c-SWNT composite. The characteristic absorption spectrum which is basically similar to those of the reported ones[47] can be clearly seen at a wavelength between 800 and 1400 nm, suggesting that SWNTs can be well-solubilized into water by SPG. To obtain clear evidence that the β-1,3-glucans really construct a periodical helical superstructure around the bundle of c-SWNTs, we observed these composite fibrils by AFM. As shown in Fig. 15a, the surfaces of c-SWNTs themselves did not give any specific pattern. On the other hand, when a DMSO solution of s-SPG was cast on mica, we could observe a fine polymeric network structure. When c-SWNTs were dispersed with the aid of s-SPG or s-curdlan (M_w = 33 kDa) into water, the surface of the fibrils showed a periodical structure with inclined stripes (Figs. 15b–15d). In a magnified picture of these fibrils

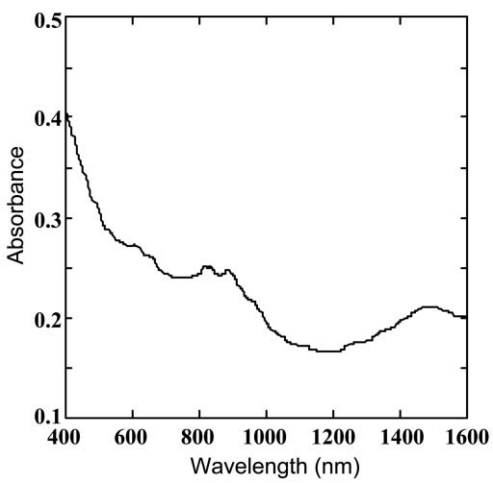

Fig. 14 VIS-NIR spectrum of c-SWNT/s-SPG solution: D_2O, 1 cm cell, room temperature. The spectrum of c-SWNT itself was almost the same as that of the c-SWNT/s-SPG composite shown above. (Adapted from ref. 38 by permission of The American Chemical Society).

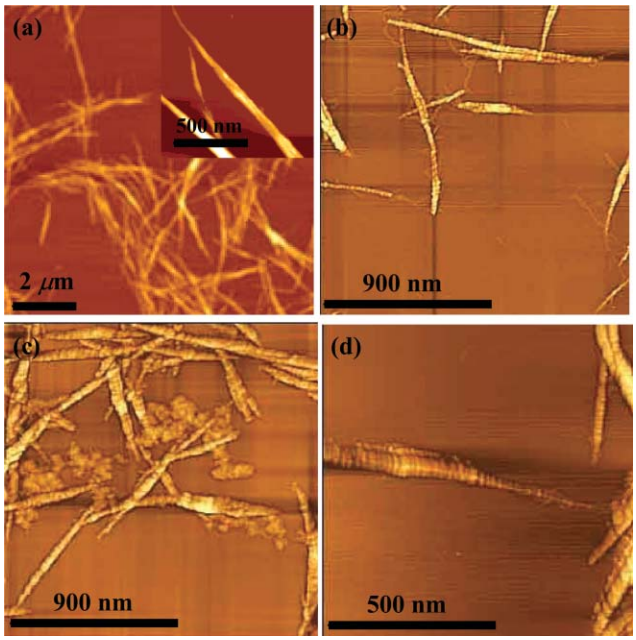

Fig. 15 AFM images of (a) c-SWNTs, (b) c-SWNTs/s-SPG composite, (c) c-SWNTs/s-curdlan composite, (d) magnified picture of fibrils in s-SWNTs/s-SPG composite. In (c), the amorphous mass observed around the fibrous composite is attributed to curdlan which could not form the composite with c-SWNTs. The same AFM image was obtained from curdlan itself. The difference in (b) and (d) is caused by poor water-solubility of curdlan. (Adapted from ref. 38 by permission of The American Chemical Society).

(Fig. 15d), one can clearly recognize that a well-ordered, periodical structure is constructed on the surface.

On the basis of these results, we prepared the sample using ag-SWNT and found that s-SPG is a remarkable solubilizer even for ag-SWNTs. ag-SWNTs were dispersed into D_2O with the aid of s-SPG and the mixture was subjected to VIS-NIR measurements (Fig. 16). The peaks have become much sharper than those of bundled c-SWNTs (Fig. 14), suggesting that one or a few pieces of ag-SWNTs are included in the SPG helical structure. The s-SPG/ag-SWNTs composite was characterized by high-resolution TEM (HRTEM).[48] It is clearly seen from Fig. 17a that the composites form very small, fibrous structures but not bundled ones. Figs. 17b and 17c are the enlarged pictures. From Fig. 17c, one can clearly see that two

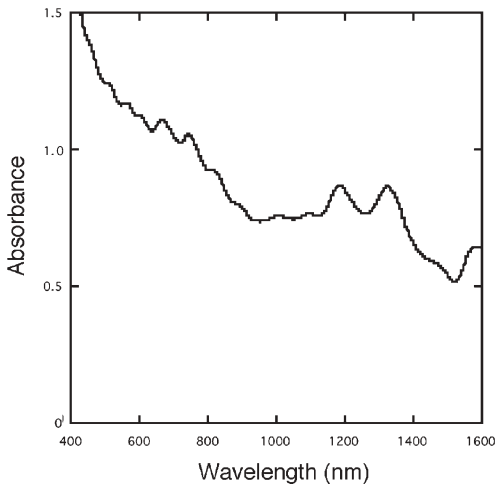

Fig. 16 VIS-NIR spectrum of ag-SWNTs/s-SPG solution: D_2O, 1 cm cell, room temperature. (Adapted from ref. 38 by permission of The American Chemical Society).

s-SPG chains twine around one ag-SWNT with 1.5 nm diameter. It is also seen from Fig. 17c that the helical motif is a right-handed one and the helical pitch of one chain is *ca.* 10 nm (in Fig. 17d, the original image is Fourier filtered to enhance the contrast of the wrapping pattern). These TEM images provide "decisive" evidence that one piece of ag-SWNTs is wrapped by s-SPG chains.[49]

Furthermore, we succeeded in taking a three-dimensional (3D) image of this picture.[50] The four selected still pictures are shown in Fig. 18. In Fig. 18, each 3D image corresponds to the clockwise rotation of the "Y" shape structure in Fig. 17b through 45°, 135°, 225° and 315° along a perpendicular axis. In these 3D images, one can easily see that ag-SWNT appears as white fine fibril (for example, right branch in the 45° rotating image) and an SPG thin layer wraps the fibril. From these 3D TEM images, one can also confirm that the s-SPG chains exist as a uniform layer around one or two pieces of ag-SWNTs, and the composite structure can be viewed from any angle. This result strongly supports the fact that s-SPG *wraps* one piece of ag-SWNT.

Various spectroscopic measurements and microscopic observations conducted herein consistently support the view that the water-soluble nanofibers are comprised of the SWNTs and the

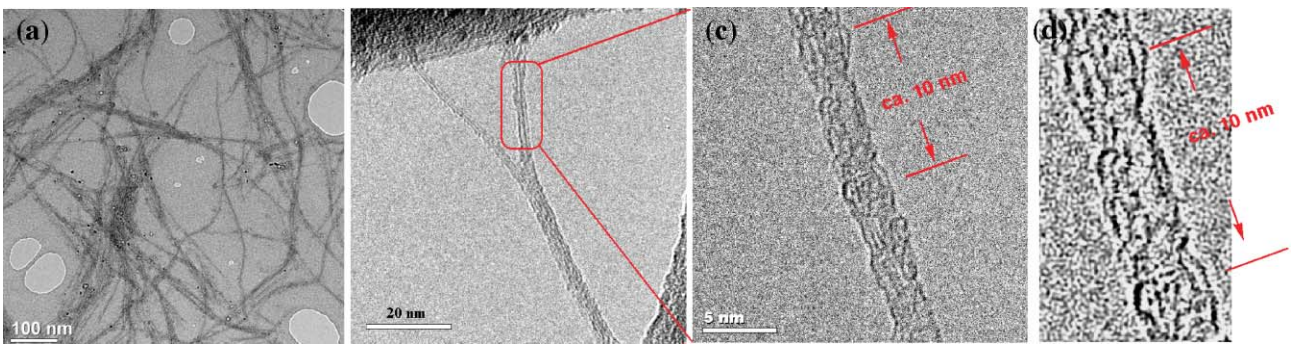

Fig. 17 (a) TEM image of ag-SWNT/s-SPG composite and (b), (c) its magnified picture. (d) The original image of (c) was Fourier filtered to enhance the contrast of the composite. (Adapted from ref. 38 by permission of The American Chemical Society).

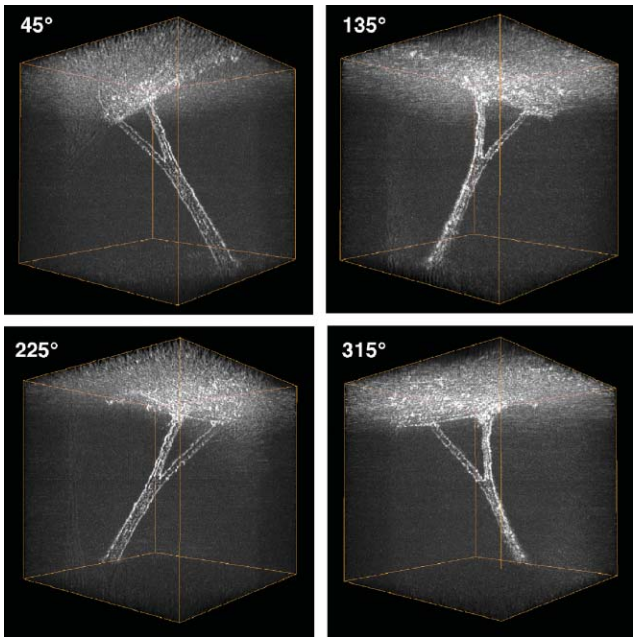

Fig. 18 Reconstructed 3-D images of ag-SWNTs/s-SPG composite, viewed from different orientations. These correspond to the clockwise rotation images of the 2-D image in Fig. 17b, rotating around a perpendicular axis through 45°, 135°, 225° and 315°, respectively. (Adapted from ref. 38 by permission of The American Chemical Society).

β-1,3-glucans. Particularly interesting are the findings that 1) the periodical stripe structure, which stems from a helical wrapping mode characteristic of the β-1,3-glucans, is confirmed, 2) the s-SPG/ag-SWNTs composite contains mainly one piece of ag-SWNT and 3) the "important" picture which is clear evidence that two s-SPG chains helically wrap one piece of ag-SWNT and the helicity is a right-handed one has been taken.

The present results show that the polymer wrapping with the β-1,3-glucans is one promising method to solubilize SWNTs, although it has not been easy so far to prepare a stable composite including one piece of SWNT isolated from the others. In addition to the unique ability to give stable composites with SWNTs, the β-1,3-glucans have various advantages for their future applications. For example, β-1,3-glucans having various functional appendages can be easily prepared and they can be used for the composite formation. Furthermore, the β-1,3-glucan main chain is highly stable in the human body because of the lack of mammalian β-1,3-glucanase. We believe, therefore, that the present system has a broad future potential both in chemical modification and physical characterization of SWNTs.

5.2 Inclusion of PANIs[51]

Polyaniline (PANI) is one of the most promising conductive polymers owing to its high chemical stability, high conductivity and unique redox properties.[52,53] In spite of these advantages, PANI and its derivatives are hardly applicable for conductive nanowires since these PANIs tend to form amorphous aggregates composed of highly entangled polymeric strands. Much research effort has been therefore devoted to the fabrication of PANI nanofibers composed of parallel-aligned strands to show excellent conductivity through the nanofibers.[54] Increasing research effort has been applied to the development of such PANI nanofibers.[55–57]

Such PANI nanofibers can easily be obtained by using SPG as a 1D host. For example, highly water-soluble SPG/PANIs nanocomposites can be obtained through gradual water-dilution of a DMSO solution containing both commercially available PANI (emerardine base, M_w = 10 kDa) and s-SPG (M_w = 150 kDa) followed by purification through repeated centrifugations (7000 rpm, 1 h, 3 times). TEM observations showed the formation of fibrous architectures from SPG/PANIs nanocomposites whose lengths were consistent with that of the SPG used (Fig. 19). The diameter of the smallest fiber is estimated to be around 10 nm, indicating that several PANI strands are co-entrapped within the 1D cavity of SPG. Together with a tight packing of PANI strands in the nanocomposites confirmed by UV-VIS spectra, these TEM images clearly indicate that SPG accommodates PANIs strands in a parallel fashion to fabricate PANI nanofibers. No such fibrous structure can be obtained by using other polysaccharides such as amylose, dextran and pullulan.

This unique strategy is also applicable to develop PANI nanofibers having specific lectin affinity by using α-mannoside-modified SPG as a 1D host. Confocal laser scanning microscopic (CLSM) observations using FITC-labeled Concanavalin A (α-mannoside-binding lectin) clearly indicate that the resultant nanocomposites have a specific lectin affinity that is advantageous for further applications toward PANI-based sensory devices (Fig. 20).

5.3 Complexation with polythiophene[58]

As described in section 5.2, the strong aggregation tendency of conductive polymers both in solution and solid phases makes it a challenging subject to fabricate conductive polymer-based molecular wires on a single-molecular scale. Hitherto, several intriguing strategies have been developed to solve this problem by designing insulated molecular wires through covalent or noncovalent approaches, in which the conductive polymer backbones are encapsulated by various protective sheaths.[59–65] Composite formation between SPG and

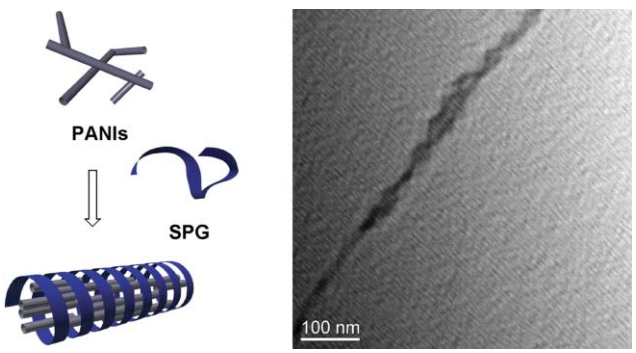

Fig. 19 (Left) Schematic illustration of the encapsulation of PANI strands within the 1D cavity of SPG to produce fibrous SPG/PANI nanocomposites and (right) TEM image of the resultant nanocomposites without staining.

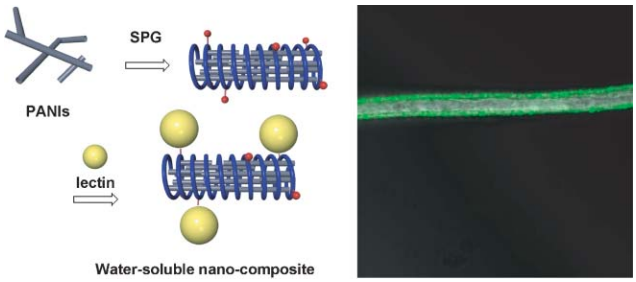

Fig. 20 (Left) Schematic illustration of the interaction between the mannoside-appended nanofibers and ConA and (right) CLSM image of the nanocomposites after incubation with FITC-ConA: optical and fluorescent images are superimposed.

conjugated polymers[66–70] was very clearly observed for polythiophene. In this case, cationic and water-soluble polythiophene (PT) (for its structure see Fig. 21) was used for the composite formation. The polycationic nature of PT and the resultant weakened inter-stranded packing result in a well-characterized SPG/PT complex, in which only one PT strand is encapsulated within the 1D cavity of SPG (Fig. 21a). CD spectra of the composites show an intense split-type induced CD (ICD) in the π–π* transition region, clearly indicating that the PT strands are chirally twisted in an intra-stranded manner in the 1D cavity of SPG. The shape and sign of the ICD pattern are characteristic of a right-handed helical structure of the PT backbones, reflecting the right-handed helical structure of SPG.

The UV-VIS spectrum of the resultant SPG/PT composites shows an absorption maximum at 454 nm that is significantly red-shifted from that (403 nm) of free PT (Fig. 21b). This distinct red-shift should arise from an SPG-induced planar conformation of the PT backbone. The emission maximum (561 nm) of SPG/PT composites is also red-shifted from that (520 nm) of free PT and slightly increases in intensity, again indicating that the PT backbones become more planar and more isolated and that the insulated molecular wire is formed during the complexation. It should be of interest that no further red shift of the absorption peaks is observed for the cast films of SPG/PT, suggesting that this PT molecular wire is still insulated even in its solid phase owing to a rigid helical superstructure of SPG surrounding the insulated PT nanowire.

5.4 As a 1D host for diacetylene polymerization[71]

The application of SPG as a 1D host can be expanded toward various non-polymeric guests including small molecular weight compounds as well as inorganic nanoparticles. For example, 1,4-bis(*p*-propionamidophenyl)butadiyne (DPB) can be accommodated within the 1D cavity through a protocol similar to that for the aforementioned polymeric guests (PANI and PT). The resultant SPG/DPB complex showed a negative CD exciton-coupling, indicating twisted-conformations or -packings of DPB within the 1D cavity of SPG. Of great interest is the finding that the resultant DPB in the 1D cavity can be polymerized through UV-irradiation (Fig. 22), demonstrating the application of SPG as a "1D template" for polymerization. For example, UV-irradiation of the SPG/DPB in aqueous DMSO using a high pressure Hg lamp induced its gradual colour change from colourless to pale blue. The UV-VIS spectrum of the resultant solution shows an absorption band at around 720 nm which is characteristic of poly(diacetylene)s with extremely long π-conjugated length and/or tight inter-stranded packings.[72,73] UV-mediated polymerization of DPB was also confirmed by Raman spectra, in which the SPG/DPB composite shows a clear peak at 2000 cm^{-1}

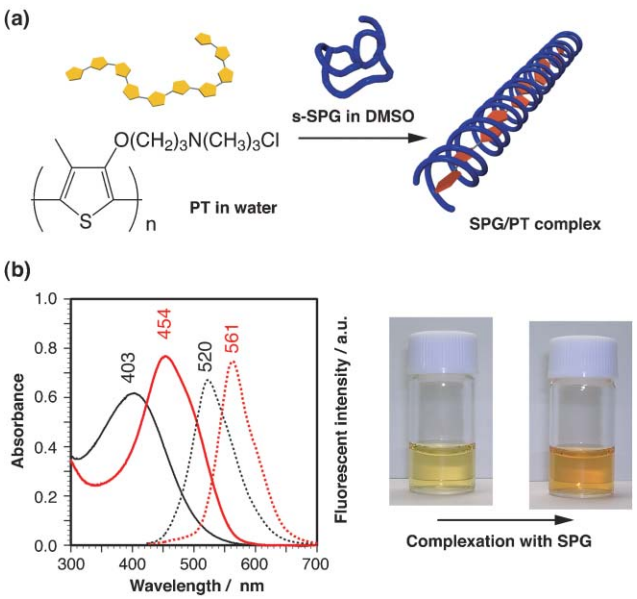

Fig. 21 (a) Schematic illustration of the composite formation between cationic polythiophene (PT) and s-SPG and (b) UV-VIS (solid lines, left *y* axis) and emission (dashed lines, right *y* axis) spectra of PT in the presence (red lines) and the absence (black lines) of s-SPG: Ex. = 400 nm.

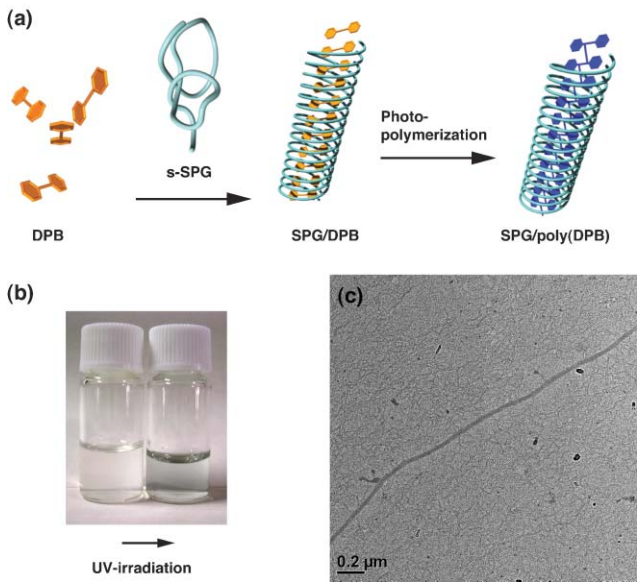

Fig. 22 (a) Schematic illustration of our concept to use SPG as a 1-D template to construct poly(diacetylene) nanofibers, (b) image of aqueous DMSO solutions containing SPG/DPB (left) before and (right) after UV-irradiation and (c) TEM image of the resultant SPG/poly(DPB)s composites without staining.

assignable to poly(diacetylene)s (–CH=CH– stretching vibration) after 16 h UV-irradiation.[73]

TEM observations of the resultant SPG/poly(DPB)s composite showed formation of the fibrous structure with diameters ranging from 2 to 20 nm. It should be again noted that no such fibrous assembly was observed for other polysaccharides, clearly emphasizing an advantage of SPG as the 1D template to produce the nanofibers. The fabrications of poly(diacetylene)-nanofibers have received increasing research interest, however, these researches mostly utilize amphiphilic diacetylene monomers that are self-assembled into rod-like assemblies. The structural properties (shapes, diameters, *etc.*) of poly(diacetylene)-nanofibers highly depend on the structure of the corresponding monomers.[74–77] On the other hand, poly(diacetylene)-nanofibers with almost uniform diameters are obtained from various DPB-derivatives.

5.5 1D arrangement of Au nanoparticles[78]

The unique renaturation process during the guest encapsulations provides one great advantage of SPG, that is, a flexible (or induced-fit-type) size/shape-selectivity for the guests. It is a clear contrast to cyclodextrins with a rigid closed ring-like structure resulting in a severe size/shape-selectivity. This advantage of SPG is clearly demonstrated by using Au nanoparticles as a large inorganic guest. For example, stable SPG/Au composites were obtained from commercially available Au nanoparticles (5–50 nm). The resultant SPG/Au composites are highly soluble in water but show significantly broadened plasmon absorption, indicating SPG-induced assemblies of Au nanoparticles in aqueous media. TEM observations of the resultant SPG/Au composites showed unique 1D Au nanoarrays with their length consistent with that of s-SPG itself ($\sim$200 nm). These data clearly indicate that the 1D nanoarrays of Au nanoparticles arise from their encapsulation within the 1D cavity of SPG (Fig. 23). It should be again emphasized that no such Au nanoarray can be developed with other polysaccharides.

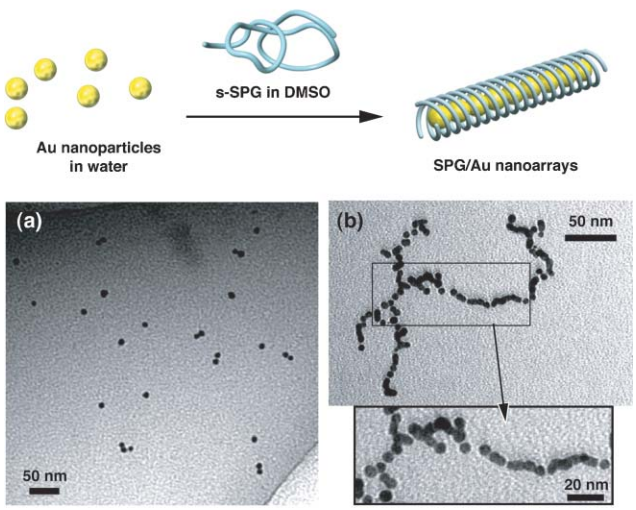

Fig. 23 TEM images of (a) free Au nanoparticles and (b) the SPG–Au nanocomposites without staining.

Nano-scale assemblies of inorganic materials have received considerable attention in recent years due to their potential as novel functional materials.[79–82] Especially, metal nano-assemblies in a desired architecture are indispensable for nanotechnologies.[83,84] We believe that our system will provide a new strategy toward nanosensors, nanowires, nanocircuits, and others.

6 Conclusions

We have demonstrated that the β-1,3-glucans have unique features that are greatly different from those of other polysaccharides. These features mostly stem from their strong helix-forming nature and reversible interconversion between single-strand random coil and triple-strand helix. During this interconversion process, they can accept certain DNAs or RNAs because the helical sense and pitch of β-1,3-glucans are complementary to those of DNAs or RNAs. The resultant macromolecular complexes have well-defined helical superstructures composed of two polysaccharide-strands and one polynucleotide-strand. Furthermore, the β-1,3-glucans can also interact with conjugate polymers, nanoparticles, *etc.* through the interconversion process to fabricate their one-dimensional assemblies. These composite formations arise from encapsulations of these guest molecules within the 1D hollow constructed by the helical superstructure of β-1,3-glucans.

So far, most polymer–polymer interactions, except those occurring in biological systems, have been considered to take place in a random fashion and to produce morphologically-uninteresting polymer-aggregates. In contrast, it is clear that the interactions with β-1,3-glucans occur in a specific fashion and construct helical (with DNAs and RNAs) or one-dimensional (with single-walled carbon nanotubes, conjugated polymers, nanoparticles, *etc.*) superstructures. Consequently, we trust that the β-1,3-glucans are unique 1D hosts for gene carriers, nanowire factories, *in situ* polymerization, *etc.*

Acknowledgements

We thank Mitsui Sugar Co., Japan, for providing SPG samples. This work was supported by the SORST Program of the Japan Science and Technology Agency.

Notes and references

1 C. Hobbs, *Medical Mushrooms*, Botanical Press, Tokyo, 1991.
2 G. Chihara, Y. Maeda, J. Hamuro, T. Sasaki and F. Fukuoka, *Nature*, 1969, **222**, 687.
3 K. Tabata, W. Ito, T. Kojima, S. Kawabata and A. Misaki, *Carbohydr. Res.*, 1981, **89**, 121.
4 T. Suzuki, A. Tsuzuki, N. Ohno, Y. Ohshima, Y. Adachi and T. Yadomae, *Biol. Pharm. Bull.*, 2002, **25**, 140.
5 K. Takeda and S. Akira, *Int. Immunol.*, 2005, **17**, 1.
6 S. H. Young, J. Ye, D. G. Frazer, X. Shi and V. Castranova, *J. Biol. Chem.*, 2001, **276**, 20781.
7 E. D. T. Atkins and K. D. Parker, *Nature*, 1968, **220**, 784.
8 Y. Deslandes, R. H. Marchessault and A. Sarko, *Macromolecules*, 1980, **13**, 1466.
9 T. Blehm and A. Sarko, *Can. J. Chem.*, 1977, **55**, 293.
10 T. Yanaki, T. Norisuye and H. Fujita, *Macromolecules*, 1980, **13**, 1462.

11 T. Norisuye, T. Yanaki and H. Fujita, *J. Polym. Sci., Polym. Phys. Ed.*, 1980, **18**, 547.
12 Y. Kashiwagi, T. Norisuye and H. Fujita, *Macromolecules*, 1981, **14**, 1220.
13 S. Sato, K. Sakurai, T. Norisuye and H. Fujita, *Polym. J.*, 1983, **15**, 87.
14 B. T. Stokke, A. Elgsaeter, D. A. Brant, T. Kuge and S. Kitamura, *Biopolymers*, 1993, **33**, 193.
15 T. M. McIntire and D. A. Brant, *J. Am. Chem. Soc.*, 1998, **120**, 6909.
16 K. Miyoshi, K. Uezu, K. Sakurai and S. Shinkai, *Chem. Biodiversity*, 2004, **1**, 916.
17 Y. Deslandes, R. H. Marchessault and A. Sarko, *Macromolecules*, 1980, **13**, 1466.
18 K. Sakurai and S. Shinkai, *J. Am. Chem. Soc.*, 2000, **122**, 4520.
19 K. Sakurai, M. Mizu and S. Shinkai, *Biomacromolecules*, 2001, **2**, 641.
20 K. Miyoshi, K. Uezu, K. Sakurai and S. Shinkai, *Biomacromolecules*, 2005, **6**, 1540.
21 K. Koumoto, T. Kimura, H. Kobayashi, K. Sakurai and S. Shinkai, *Chem. Lett.*, 2001, 908.
22 W. Saenger, *Principles of Nucleic Acid Structure*, (Springer-Verlag, New York; 1984).
23 R. Karinaga, M. Mizu, K. Koumoto, T. Anada, T. Kimura, T. Kimura, S. Shinkai and K. Sakurai, *Chem. Biodiversity*, 2004, **1**, 603.
24 T. Kimura, A. Beppu, K. Sakurai and S. Shinkai, *Biomacromolecules*, 2005, **6**, 174.
25 A. M. Krieg, *Biochim. Biophys. Acta*, 1999, **1489**, 107.
26 H. Henmi, O. Takeuchi, T. Kawai, T. Kaisho, S. Sato, H. Sanjo, M. Matsumoto, K. Hoshino, H. Wagner, K. Takeda and S. Akira, *Nature*, 2000, **408**, 740.
27 P. Ahmad-Nejad, H. Hacker, M. Rutz, S. Bauer, R. M. Vabulas and H. Wagner, *Eur. J. Immunol.*, 2002, **32**, 1958.
28 C. A. Stein and Y. C. Cheng, *Science*, 1993, **261**, 1004.
29 T. V. Chirila, P. E. Rakoczy, K. L. Garrett, X. Lou and I. J. Constable, *Biomaterials*, 2002, **23**, 321.
30 T. Matsumoto, M. Numata, T. Anada, M. Mizu, K. Koumoto, K. Sakurai, T. Nagasaki and S. Shinkai, *Biochim. Biophys. Acta*, 2004, **1670**, 91.
31 K. Koumoto, T. Kimura, M. Mizu, K. Sakurai and S. Shinkai, *Chem. Commun.*, 2001, 1962.
32 M. Mizu, K. Koumoto, T. Anada, K. Sakurai and S. Shinkai, *Biomaterials*, 2004, **25**, 3117.
33 M. Mizu, K. Koumoto, T. Kimura, K. Sakurai and S. Shinkai, *Biomaterials*, 2004, **25**, 3109.
34 M. Mizu, K. Koumoto, T. Anada, T. Matsumoto, M. Numata, S. Shinkai, T. Nagasaki and K. Sakurai, *J. Am. Chem. Soc.*, 2004, **126**, 8372.
35 T. Hasegawa, T. Fujisawa, S. Haraguchi, M. Numata, R. Karinaga, T. Kimura, S. Okumura, K. Sakurai and S. Shinkai, *Bioorg. Med. Chem. Lett.*, 2005, **15**, 327.
36 R. Karinaga, K. Koumoto, M. Mizu, T. Anada, S. Shinkai and K. Sakurai, *Biomaterials*, 2004, in press.
37 For carbohydrate nanotubes formed by cyclodextrins or their analogues, for example see: (*a*) G. Li and L. B. McGown, *Science*, 1994, **264**, 249; (*b*) G. Gattuso, S. Menzer, S. A. Nepogodiev, J. F. Stoddart and D. J. Williams, *Angew. Chem., Int. Ed.*, 1997, **36**, 1451; (*c*) P. R. Ashton, S. J. Cantrill, G. Gattuso, S. Menzer, S. A. Nepogodiev, A. N. Shipway, J. F. Stoddart and D. J. Williams, *Chem. Eur. J.*, 1997, **3**, 1299; (*d*) A. Harada, *Acc. Chem. Res.*, 2001, **34**, 456; (*e*) T. Michishita, M. Okada and A. Harada, *Macromol. Rapid Commun.*, 2001, **22**, 763; (*f*) H. Okumura, Y. Kawaguchi and A. Harada, *Macromolecules*, 2003, **36**, 6422.
38 (*a*) M. Numata, M. Asai, K. Kaneko, T. Hasegawa, N. Fujita, Y. Kitada, K. Sakurai and S. Shinkai, *Chem. Lett.*, 2004, **33**, 232; (*b*) M. Numata, M. Asai, K. Kaneko, A.-H. Bae, T. Hasegawa, K. Sakurai and S. Shinkai, *J. Am. Chem. Soc.*, 2005, **127**, 5875.
39 (*a*) S. Iijima, *Nature*, 1991, **354**, 56; (*b*) S. Iijima and T. Ichihashi, *Nature*, 1993, **363**, 603; (*c*) D. S. Bethune, C. H. Kiang, M. S. de Vries, G. Gorman, R. Savoy and J. Savoy, *Nature*, 1993, **363**, 605.
40 (*a*) P. M. Ajayan, *Chem. Rev.*, 1999, **99**, 1787; (*b*) P. M. Ajayan and O. Z. Zhou, *Top. Appl. Phys.*, 2001, **80**, 391; (*c*) A. Hirsch, *Angew. Chem., Int. Ed.*, 2002, **41**, 1853; (*d*) H. Dai, *Acc. Chem. Res.*, 2002, **35**, 1035; (*e*) S. Niyogi, M. A. Hamon, H. Hu, B. Zhao, P. Bhowmik, R. Sen, M. E. Itkis and R. C. Haddon, *Acc. Chem. Res.*, 2002, **35**, 1105; (*f*) S. Banerjee, M. G. C. Kahn and S. S. Wong, *Chem. Eur. J.*, 2003, **9**, 1898; (*g*) C. A. Dyke and J. M. Tour, *Chem. Eur. J.*, 2004, **10**, 812.
41 (*a*) S. J. Tans, M. H. Devoret, H. Dai, A. Thess, R. E. Smalley, L. J. Geerligs and C. Dekker, *Nature*, 1997, **386**, 474; (*b*) S. J. Tans, A. R. M. Verschnesen and C. Dekker, *Nature*, 1998, **393**, 49; (*c*) S. J. Tans and C. Dekker, *Nature*, 2000, **404**, 834; (*d*) S. G. Louie, *Top. Appl. Phys.*, 2001, **80**, 113; (*e*) B. I. Yakobson and P. Avouris, *Top. Appl. Phys.*, 2001, **80**, 287; (*f*) M. Ouyang, J.-L. Huang and C. M. Lieber, *Acc. Chem. Res.*, 2002, **35**, 1018; (*g*) R. H. Baughman, A. A. Zakhidov and W. A. de Heer, *Science*, 2002, **297**, 787; (*h*) T. Fukushima, A. Kosaka, Y. Ishimura, T. Yamamoto, T. Takigawa, N. Ishii and T. Aida, *Science*, 2003, **300**, 2072.
42 For DNA, see: (*a*) M. Zheng, A. Jagota, E. D. Semke, B. A. Diner, R. S. Mclean, S. R. Lustig and R. E. R. Tassi, *Nat. Mater.*, 2003, **2**, 338; (*b*) M. Zheng, A. Jagota, M. S. Strano, A. P. Santos, P. Barone, S. G. Chou, B. A. Diner, M. S. Dresselhaus, R. S. Mclean, G. B. Onoa, G. G. Samsonidze, E. D. Semke, M. Usrey and D. J. Walls, *Science*, 2003, **302**, 1545; (*c*) N. Nakashima, S. Okuzono, H. Murakami, T. Nakai and K. Yoshikawa, *Chem. Lett.*, 2003, **32**, 456. For peptide, see: (*d*) T. Takahashi, K. Tsunoda, H. Yajima and T. Ishii, *Chem. Lett.*, 2002, **31**, 690; (*e*) D. Pantarotto, C. D. Partidos, R. Graff, J. Hoebeke, J.-P. Briand, M. Prato and A. Bianco, *J. Am. Chem. Soc.*, 2003, **125**, 6160; (*f*) G. R. Dieckmann, A. B. Dalton, P. A. Johnson, J. Razal, J. Chen, G. M. Giordano, E. Munoz, I. H. Musselman, R. H. Baughaman and R. K. Draper, *J. Am. Chem. Soc.*, 2003, **125**, 1770; (*g*) V. Zorbas, A. Ortiz-Acevedo, A. B. Dalton, M. M. Yoshida, G. R. Dieckmann, R. K. Draper, R. H. Baughman, M. J. Yacaman and I. M. Musselman, *J. Am. Chem. Soc.*, 2004, **126**, 7222.
43 (*a*) A. Star, D. W. Steuerman, J. R. Heath and J. F. Stoddart, *Angew. Chem., Int. Ed.*, 2002, **41**, 2508; (*b*) O.-K. Kim, J. Je, J. W. Baldwin, S. Kooi, P. E. Phehrsson and L. J. Buckley, *J. Am. Chem. Soc.*, 2003, **125**, 4426. For unbundling of carbon nanotube using Gum Arabic, see: R. Bandyopadhyaya, N.-R. Einat, R. Oren and Y.-R. Rachel, *Nano Lett.*, 2002, **2**, 25.
44 A supramolecular network was made from sugar-modified SWNTs and lectin. See: (*a*) K. Matsuura, K. Hayashi and N. Kimizuka, *Chem. Lett.*, 2003, 212; (*b*) T. Hasegawa, M. Numata, T. Fujisawa, K. Sakurai and S. Shinkai, *Chem. Commun.*, 2004, 2150; (*c*) L. Gu, T. Elkin, X. Jiang, H. Li, Y. Lin, L. Qu, T.-R. J. Tzeng, R. Joseph and Y.-P. Sun, *Chem. Commun.*, 2005, 874.
45 T. M. McIntire and D. A. Brant, *J. Am. Chem. Soc.*, 1998, **120**, 6909 and references cited therein.
46 M. Sano, A. Kamino, J. Okamura and S. Shinkai, *Science*, 2001, **293**, 1299.
47 (*a*) N. Nakashima, S. Okuzono, H. Murakami, T. Nakai and K. Yoshikawa, *Chem. Lett.*, 2003, **32**, 456; (*b*) J. N. Coleman, A. B. Dalton, S. Curran, A. Rubio, A. P. Davey, A. Drury, B. McCarthy, B. Lahr, P. M. Ajayan, S. Roth, R. C. Barklie and W. J. Blau, *Adv. Mater.*, 2000, **12**, 213.
48 The electron conductivity of carbon nanotubes plays an important role in shielding the sample from electron beam damage. See: (*a*) S. C. Tsang, Z. Guo, Y. K. Chen, M. L. H. Green, H. A. O. Hill, T. W. Hambley and P. J. Sadler, *Angew. Chem., Int. Ed.*, 1997, **36**, 2197; (*b*) Z. Guo, P. J. Sadler and S. C. Tsang, *Adv. Mater.*, 1998, **10**, 701. For HRTEM recent review see: J. M. Thomas and P. A. Midgley, *Chem. Commun.*, 2004, 1253.
49 Recently, Coleman and Ferreira presented a simple and general model that describes the ordered assembly of polymer strands on nanotube surfaces, the energetically favourable coiling angles being estimated to be 48°–70°. J. N. Coleman and M. S. Ferreira, *Appl. Phys. Lett.*, 2004, **84**, 798. This theoretical approach is partly complementary to our present results, but their single chain wrapping system cannot be directly compared with our two chains wrapping system.
50 Electron tomography (ET) is a useful technique for reconstructing an object from a series of projections acquired by TEM. The recent development of fully-digitized and automated TEM has enabled us to achieve three-dimensional ET, not only to determine the size and distribution of objects but also to provide information about the morphology of them in the nanometer-order. Three-dimensional

structure was reconstructed by processing a series of projections by combination of IMOD and Amira. See: (*a*) J. Frank, *Three-dimensional Electron Microscopy of Macromolecular Assemblies*, Academic Press: San Diego, 1996; (*b*) P. Midgley and M. Weyland, *Ultramicroscopy*, 2003, **96**, 413; (*c*) J. R. Kermer, D. N. Mastronarde and J. R. McIntosh, *J. Struct. Biol.*, 1996, **116**, 71.
51 M. Numata, T. Hasegawa, T. Fujisawa, K. Sakurai and S. Shinkai, *Org. Lett.*, 2004, **6**, 4447.
52 A. G. MacDiamid, J. C. Chiang, M. Halpern, W. S. Huang, S. L. Mu, N. L. D. Somasiri, W. Wu and S. I. Yaniger, *Mol. Cryst. Liq. Cryst.*, 1985, **121**, 173.
53 A. G. MacDiamid, J. C. Chiang, A. F. Richter and A. J. Epstein, *Synth. Met.*, 1987, **18**, 285.
54 J. Huang and R. B. Kaner, *Angew. Chem., Int. Ed.*, 2004, **43**, 5817.
55 Y. Wang, Z. Liu, B. Han, Z. Sun, Y. Huang and G. Yang, *Langmuir*, 2005, **21**, 833.
56 R. Pauliukaite, C. M. A. Brett and A. P. Monkman, *Electrochim. Acta*, 2004, **50**, 159.
57 (*a*) K. Yoshida, T. Shimomura, K. Ito and R. Hayakawa, *Langmuir*, 1999, **15**, 910; (*b*) T. Shimomura, K. Yoshida, K. Ito and R. Hayakawa, *Polym. Adv. Technol.*, 2000, **11**, 837; (*c*) X. Zhang and S. K. Manohar, *Chem. Commun.*, 2004, **20**, 2360.
58 C. Li, M. Numata, A.-H. Bae, K. Sakurai and S. Shinkai, *J. Am. Chem. Soc.*, 2005, **127**, 4548.
59 J. Buey and T. M. Swager, *Angew. Chem., Int. Ed.*, 2000, **39**, 608.
60 J.-P. Sauvage, J.-M. Kern, G. Bidan, B. Divisia-Blohorn and P.-L. Vidal, *New J. Chem.*, 2002, **26**, 1287.
61 F. Cacialli, J. S. Wilson, J. J. Michels, C. Daniel, C. Silva, R. H. Friend, N. Severin, P. Samori, J. P. Rabe, N. J. O'Connell, P. N. Taylor and H. L. Anderson, *Nat. Mater.*, 2002, **1**, 160.
62 J. J. Michels, M. J. O'Connell, P. N. Taylor, J. S. Wilson, F. Cacialli and H. L. Anderson, *Chem. Eur. J.*, 2003, **9**, 6167.
63 R. E. Martin and F. Diederich, *Angew. Chem., Int. Ed.*, 1999, **38**, 1350.
64 S. Hecht and J. M. J. Fréchet, *Angew. Chem., Int. Ed.*, 2001, **40**, 74.
65 T. Sato, D.-L. Jiang and T. Aida, *J. Am. Chem. Soc.*, 1999, **121**, 10658.
66 J. M. Tour, *Chem. Rev.*, 1996, **96**, 537.
67 J. Roncali, *Chem. Rev.*, 1997, **97**, 173.
68 D. T. McQuade, A. E. Pullen and T. M. Swager, *Chem. Rev.*, 2000, **100**, 2537.
69 H.-A. Ho, M. Boissinot, M. G. Bergeron, G. Corbeil, K. Doré, D. Boudreau and M. Leclerc, *Angew. Chem., Int. Ed.*, 2002, **41**, 1548.
70 M. R. Pinto and K. S. Schanze, *Proc. Natl. Acad. Sci. USA*, 2004, **101**, 7505.
71 T. Hasegawa, S. Haraguchi, M. Numata, T. Fujisawa, C. Li, K. Kaneko, K. Sakurai and S. Shinkai, *Chem. Lett.*, 2005, **34**, 40.
72 G. Wenz, M. A. Müller, M. Schmidt and G. Wegner, *Macromolecules*, 1984, **17**, 837.
73 E. Shirai, Y. Urai and K. Itoh, *J. Phys. Chem. B*, 1998, **102**, 3765.
74 (*a*) K. Tajima and T. Aida, *Chem. Commun.*, 2000, 2399; (*b*) T. Aida and K. Tajima, *Angew. Chem., Int. Ed.*, 2001, **40**, 3803.
75 M. Masuda, T. Hanada, K. Yase and T. Shimizu, *Macromolecules*, 1998, **31**, 9408.
76 K. Morigaki, T. Baumgart, U. Jonas, A. Offenhausser and W. Knoll, *Langmuir*, 2002, **18**, 4082.
77 T. Shimizu, *Polym. J.*, 2003, **35**, 1.
78 A.-H. Bae, M. Numata, T. Hasegawa, C. Li, K. Kaneko, K. Sakurai and S. Shinkai, *Angew. Chem., Int. Ed.*, 2005, **44**, 2030.
79 A. Fu, C. M. Micheel, J. Cha, H. Chang, H. Yang and A. P. Alivisatos, *J. Am. Chem. Soc.*, 2004, **126**, 10832.
80 S.-J. Park, T. A. Taton and C. A. Mirkin, *Science*, 2002, **295**, 1503. For recent review see ref. 81.
81 (*a*) E. Katz and I. Willner, *Angew. Chem., Int. Ed.*, 2004, **43**, 6042; (*b*) N. L. Rosi and C. A. Mirkin, *Chem. Rev.*, 2005, **105**, 1547.
82 C. A. Mirkin, R. L. Letsinger, R. C. Mucic and J. J. Storhoff, *Nature*, 1996, **382**, 607.
83 (*a*) J.-M. Nam, S.-J. Park and C. A. Mirkin, *J. Am. Chem. Soc.*, 2002, **124**, 3820; (*b*) H. Li, S. H. Park, J. H. Reif, T. H. LaBean and H. Yan, *J. Am. Chem. Soc.*, 2004, **126**, 418; (*c*) Z. Deng, Y. Tian, S.-H. Lee, A. E. Ribbe and C. Mao, *Angew. Chem., Int. Ed.*, 2005, **44**, 3582.
84 (*a*) J. Yang, M. Mayer, J. K. Kriebel, P. Garstecki and G. M. Whitesides, *Angew. Chem., Int. Ed.*, 2004, **43**, 1555. For recent review see: (*b*) J. C. Love, L. A. Estroff, J. K. Kriebel, R. G. Nuzzo and G. M. Whiteside, *Chem. Rev.*, 2005, **105**, 1103.

